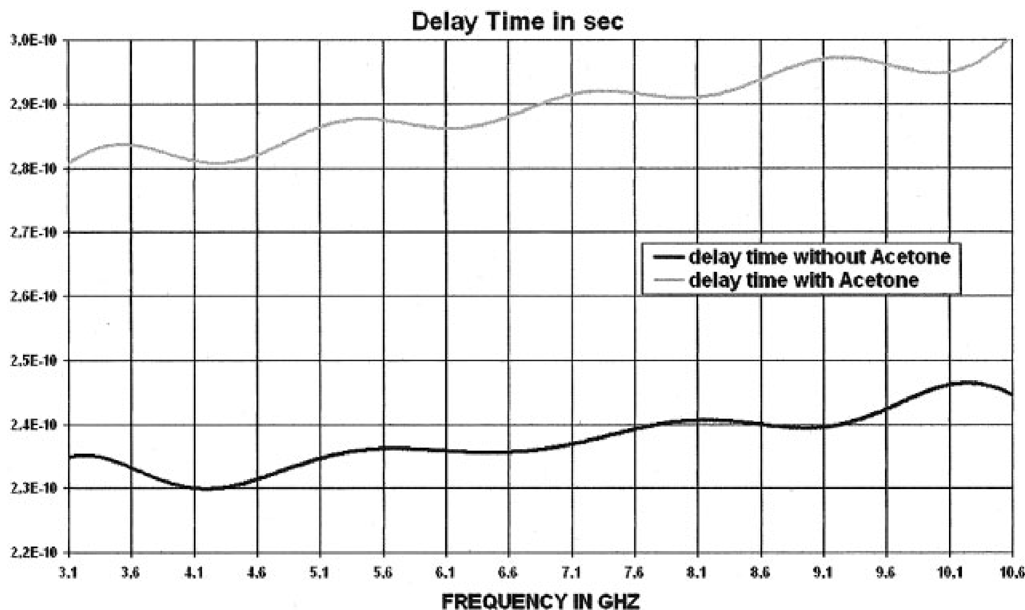

Figure 6 Computed group delay time for the 10 cells delay line device

applications in the terahertz spectra. Future works will address realization and characterization of such a system and the microfluidic management operation.

ACKNOWLEDGMENTS

This work is supported by the European Regional Development Fund and the Region Nord-Pas-de Calais.

REFERENCES

1. A. Benlarbi-Delaï and B. Bocquet, Noisy echo detection using microwave correlation radiometry, Electron Lett 38 (2002), 229–230.
2. G.M. Rebeiz, G.L. Tan, and J.S. Hayden, RF-MEMS phase shifters: design and applications, IEEE Microwave Magazine 3 (2002), 72–81.
3. L. Buchaillot, Feedback of MEMS reliability study on the design stage: a step toward reliability aided design, Microelectron Reliab 43 (2003), 1919–1928.
4. D.B. Wolf, R.S. Conroy, P. Garstecki, B.T. Mayers, M.A. Fischbach, K.E. Paul, M. Prentiss, and G.M. Whitesides, Dynamic control of liquid-core/liquid-cladding optical waveguides, Proc Natl Acad Sci USA 101 (2004), 12434–12438.
5. J.K. Young, Y.P. Jae, and U.B. Jong, Integrated RF MEMS phase shifter with constant phase shift, Conference of IEEE Microwave Theory and Techniques, Digest (2003), 1489–1492.
6. A.R. Von Hipple, Dielectric material and applications, Wiley, New York, 1954.
7. N.S. Barker and G.M. Rebeiz, Distributed MEMS true-time delay phase shifter and wide band switches, IEEE Trans Microwave Theory Tech 46 (1998), 1881–1890.
8. N. Vandelli, D. Wroblewski, M. Velonis, and T. Bifano, Development of a MEMS microvalve array for fluid flow control, IEEE J Electromech Syst 7 (1998), 395–402.
9. R.J. Yang, L.M. Fu, and Y.C. Lin, Electro-osmotic flow in microchannel, J Colloid Interface Sci 239 (2001), 98–105.

© 2006 Wiley Periodicals, Inc.

ELECTRIC STRESS EFFECT ON DC-RF PERFORMANCE DEGRADATION OF 0.18-μm MOSFETS

C. C. Chen, H. L. Kao, and Albert Chin
Institute of Electronics
National Chiao Tung University
Hsinchu, Taiwan

Received 20 March 2006

ABSTRACT: *We have studied the electric stress effect on DC-RF performance degradation of 64 gate fingers 0.18-μm RF MOSFETs. The fresh devices show good transistor's DC to RF characteristics of small sub-threshold swing of 85 mV/dec, large drive current* ($I_{d,sat}$) *of 500 μA/μm, high unity-gain cut-off frequency* (f_t) *of 47 GHz, and low minimum noise figure* (NF_{min}) *of 1.3 dB at 10 GHz. The hot carrier stress for 20%* $I_{d,sat}$ *reduction causes DC* g_m *and* r_o *degradation as well as the lower RF current gain by 2.35 dB,* f_t *reduction to 35.7 GHz, increasing* NF_{min} *to 1.7 dB at 10 GHz and poor output impedance matching.*

© 2006 Wiley Periodicals, Inc. Microwave Opt Technol Lett 48: 1916–1919, 2006; Published online in Wiley InterScience (www.interscience.wiley.com). DOI 10.1002/mop.21813

Key words: *stress; I–V; current gain; S parameters;* NF_{min}

1. INTRODUCTION

The sub-micron Si MOSFETs [1–8] have been widely used for wireless communication due to the relative low cost, high integration capability with base band, and reasonable good RF noise and gain performance. However, the degradation of RF performance for Si MOSFETs under the continuous operation is a key issue for RF ICs [1–4]. The degradation is more severe for RF ICs than digital and analog counterparts due to the tight circuit requirements on impedance matching, low RF noise, and high gain [7]. Therefore, it is necessary to understand the transistor's RF performance degradation and its relation to DC case under continuous operation and stress condition. In this study, we have first stressed the

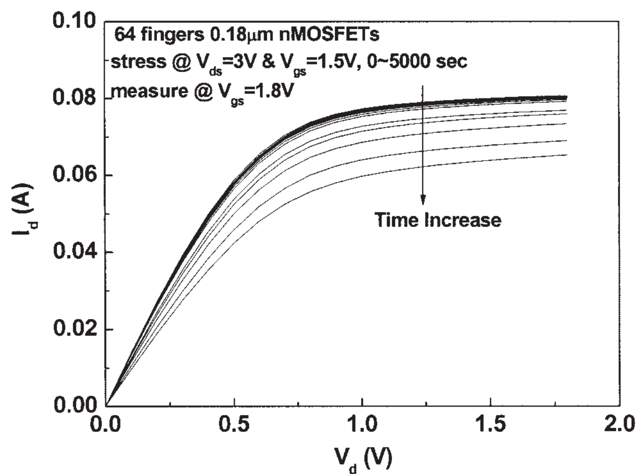

(a)

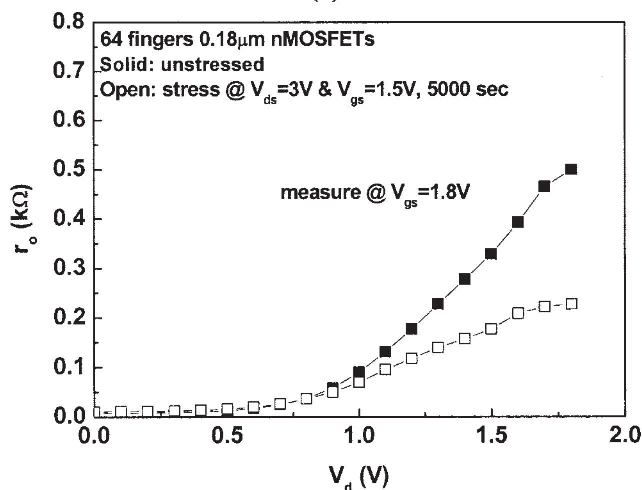

(b)

Figure 1 Measured (a) I_d–V_d and (b) r_o–V_d curves of the 64 gate fingers 0.18-μm RF MOSFETs under hot carrier stress from 0 to 5000 s

0.18-μm MOSFETs to give a ~20% reduction in drive current (equivalent to 12.5 years continuous operation at 1.8 V). Significant RF performance degradation was measured: at 10 GHz, the low minimum noise figure (NF_{min}) increases by 0.4–0.5 dB and $H_{21}{}^2$ decreases by 2.35 dB. The S_{22} change was also found that will cause impedance mismatch and gain reduction in RF IC. Such S_{22} change is due to the unavoidable reduction of output impedance (r_o) after stress. From the analysis of derived NF_{min} equation [5], the increasing NF_{min} after stress is mainly due to the decreased unity-gain cut-off frequency (f_t) from 47 to 35.7 GHz. These RF performance degradations under continuous stress operation should be considered during circuit design.

2. DESIGN AND FABRICATION

To reduce the gate-resistance generated, thermal noise at RF regime, 64 parallel gate-fingers 0.18-μm nMOSFETs with 2.5 μm finger width were used in this study [5–8]. The devices were fabricated in an IC foundry on the VLSI-standard low resistivity (10 Ω cm) Si substrate. To screen out the RF noise generation from the low resistivity substrate network [8, 9], a microstrip transmission line layout was designed instead of a conventional coplanar waveguide (CPW) structure [8]. The fabricated 64 gate fingers 0.18-μm MOSFETs were then stressed at V_{ds} = 3 V and V_{gs} = 1.5 V [10, 11] from 0 to 5000 s. The fresh and stressed devices were characterized by DC I–V, S-parameters, and NF_{min} measurements to 18 GHz using HP4155C, HP8510C network analyzer, and ATN-NP5B noise parameter system, respectively.

3. EXPERIMENTAL RESULTS AND DISCUSSION

Figure 1(a) shows the I_d–V_d characteristics of 64 gate fingers 0.18-μm MOSFETs under V_{gs} = 0.5, V_{ds} = 1.5 V stress from 0 to 5000 s. The I_d degrades monotonically with increasing stress time of the 0.18 μm devices, which is due to the generation of interface traps and decreased electron mobility [10, 11]. The stress condition gives a 20% reduction of saturation drain current ($I_{d,sat}$) after hot carrier stress. In addition to the decreased drive current, the r_o shown in Figure 1(b), from the inverse derivative of I_d–V_d at saturation region, is also reduced by 54%. Such decreased r_o will also decrease the RF voltage gain and cause output mismatch in a circuit (shown in the S_{22} plot of Fig. 4).

Figure 2(a) shows the I_d–V_g characteristics of 64 gate fingers 0.18-μm MOSFETs under the worse hot carrier stress condition of V_{ds} = 3 V and V_{gs} = 1.5 V stress from 0 to 5000 s. The small sub-threshold swing (SS) of 85 mV/dec, large drive current of 500 μA/μm, and small threshold voltage (V_{th}) of 0.47 V indicate the

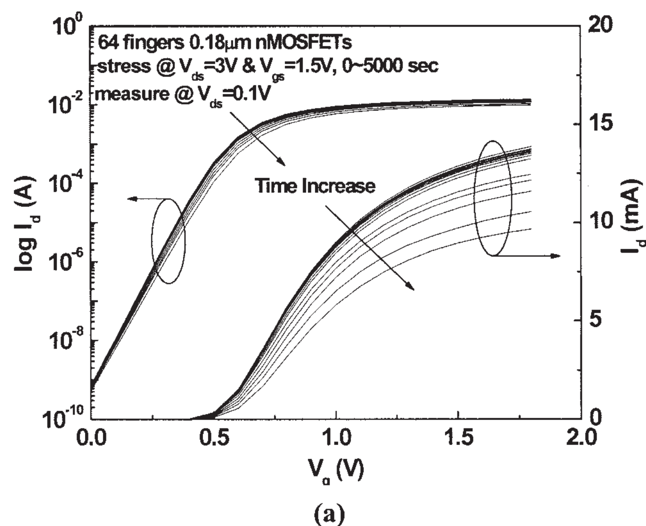

(a)

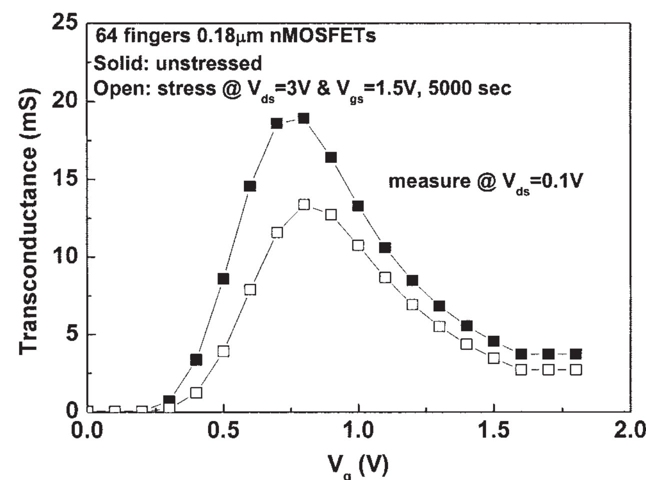

(b)

Figure 2 Measured (a) I_d–V_g and (b) g_m–V_g curves of the 64 gate fingers 0.18-μm RF MOSFETs under hot carrier stress from 0 to 5000 s

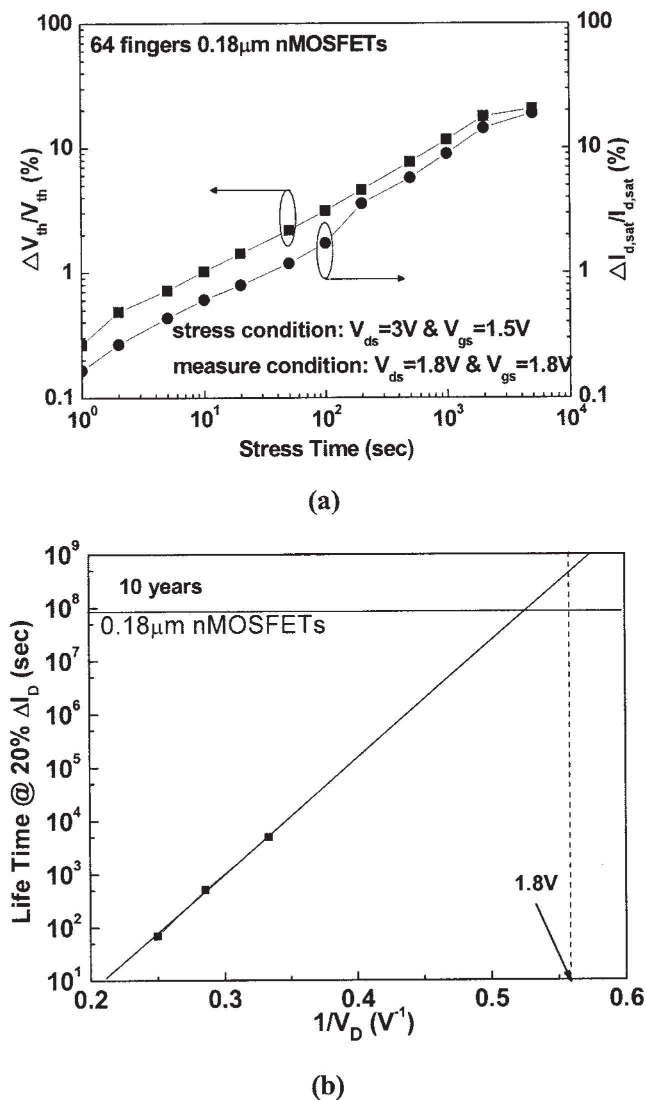

Figure 3 (a) Time dependence of $I_{d,sat}$ and Vth degradation and (b) the lifetime for 64 gate fingers 0.18-μm RF MOSFETs

good transistor's DC characteristics. Both the V_{th} and SS degrade continuously with increasing stress time, which is consistent with the I_d–V_d degradation trend. Figure 2(b) shows the trans-conductance (g_m) versus V_g plots before and after hot carrier stress. Such g_m degradation is also due to the mobility degradation by hot carrier stress [10, 11], which was originated from the hot electron-induced interface state and oxide charge near the drain side.

Figure 3(a) summarizes the time dependence of $\Delta I_{d,sat}/I_{d,sat}$ and $\Delta V_{th}/V_{th}$ of 64 gate fingers 0.18-μm RF MOSFETs under hot carrier stress of V_{gs} = 0.5 V, V_{ds} = 1.5 V from 0 to 5000 s. The $I_{d,sat}$ and V_{th} degradation with increasing stress time follows the typical power laws ($\propto t^n$) and shown as a straight line in the log plot of $\Delta I_{d,sat}/I_{d,sat}$ and $\Delta V_{th}/V_{th}$, versus stress time. Such stress gives ~20% degradation of both $I_{d,sat}$ and V_{th}. To further investigate the equivalent stress to continuous operation at 1.8 V, we have stressed the 0.18-μm RF MOSFETs under different stress voltage. Figure 3(b) shows the lifetime as a function of stress voltage, where the lifetime is defined under the criteria of 20% $I_{d,sat}$ reduction. From the I/V_d extrapolation, the accelerated stress at V_{gs} = 1/2 V, V_{ds} = 1.5 V for 5000 s is equivalent to a continuous 10 years operation at 1.81 V or 12.5 years operation at 1.8 V.

Figure 4(a) shows the measured S-parameters of 64 gate fingers 0.18-μm RF MOSFETs before and after hot carrier stress. The S_{11} and S_{12} only show slight degradation after hot carrier stress due to the small change related to each capacitance. In contrast, significant degradation of S_{21} (divided by 6 to fit in the Smith chart) and S_{22} are observed after hot carrier stress. The degradation of S_{22}, shown as a reduced output resistance in Smith chart, is consistent with the decreased r_o in I_d–V_d characteristics, which will cause output impedance mismatch of a circuit. The degraded S_{21} is due to the decreased RF gain from the lower g_m after stress. Such effect can be seen clearer in the RF current gain ($|H_{21}|^2$) as a function of frequency plot shown in Figure 4(b). The ($|H_{21}|^2$) of 64 gate fingers 0.18-μm RF MOSFETs follows the typical −20 dB/dec slope before and after stress, but the hot carrier stress lowers the ($|H_{21}|^2$) gain by 2.35 dB. Similar reduction of power gain (G_{max}) by 2.0 dB was also found after stress with little change in the −10 dB/dec slope. After hot carrier stress, the f_t extrapolated from the ($H_{21}{}^2$) curve decreases from 47 to 35.7 GHz. The f_t degradation rate is 23% and close to the $I_{d,sat}$ degradation rate, which is mainly due to the g_m reduction.

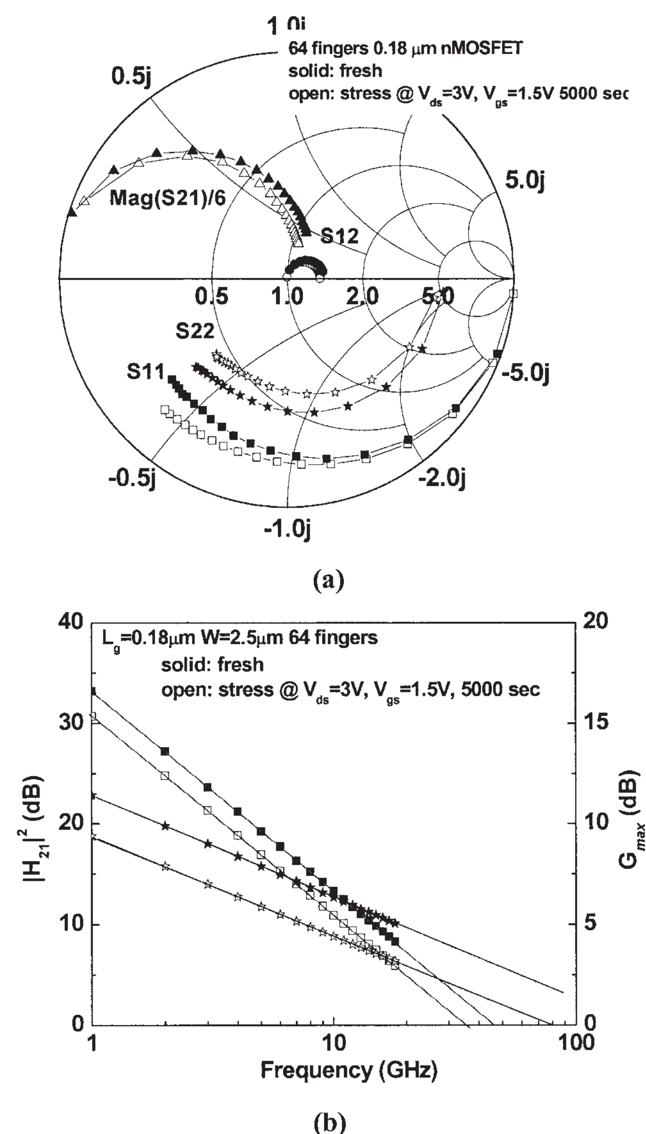

Figure 4 Measured (a) S-parameters and (b) RF current gain $H_{21}{}^2$ and G_{max} as a function of frequency of 64 gate fingers 0.18-μm RF MOSFETs before and after hot carrier stress

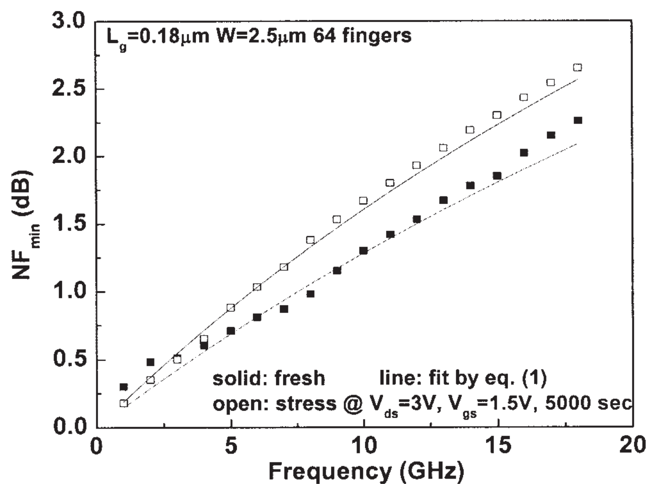

Figure 5 Measured and calculated NF_{min} of 64 gate fingers 0.18-μm RF MOSFETs before and after hot carrier stress

Figure 5 shows the NF_{min} as a function of frequency of 64 gate fingers 0.18-μm RF MOSFETs before and after hot carrier stress. At 10 GHz, useful for ultra-wide band (3.1–10.6 GHz) communication, the hot carrier stress increases NF_{min} from 1.3 to 1.7 dB, which is significant for low noise amplifier. Such increase of NF_{min} is mainly due to the decreased f_t by following equation [7]:

$$NF_{min} = 1 + 2\gamma(1 + g_m R_g/\gamma)^{1/2} f/f_t. \quad (1)$$

The γ is the drain current noise correlation factor, which has an ideal value of 0.67 [12]. By inserting the measured g_m and f_t in above equation with γ keeping constant to be 0.7, good agreement between measured and calculated NF_{min} is obtained for the 0.18 μm devices before and after hot carrier stress (see Fig. 5). Although the stress also causes the decreased g_m, the $g_m R_g/\gamma$ term in NF_{min} equation is smaller than 1 and less significant than the f_t reduction.

4. CONCLUSION

We have investigated the hot carrier stress effect to the DC and RF performance degradation of 64 gate fingers 0.18-μm RF MOSFETs. Under a failure criteria of 20% $I_{d,sat}$ reduction after stress, the DC g_m and r_o are also degraded. The stress causes RF current gain and f_t decreases and increases the undesired NF_{min} with poorer output impedance matching. All these effects should be considered during RF circuit design.

ACKNOWLEDGMENT

The coauthor Albert Chin would like to acknowledge the help from Director and Prof. Tsu-Jae King at EECS, UC-Berkeley. This work has been supported by NSC (94–2215-E-009–062).

REFERENCES

1. Q. Li, J. Zhang, W. Li, J.S. Yuan, Y. Chen, and A.S. Oates, RF circuit performance degradation due to soft breakdown and hot carrier effect in 0.18 μm CMOS technology, Digest of Papers-IEEE Radio Frequency Integrated Circuits (RFIC) Symposium (2001), 139–142.
2. J.P. Walko and B. Abadeer, RF-S-parameter degradation under hot carrier stress, IEEE Int Reliability Phys Symp Proc (2004), 422–425.
3. E. Xiao, J.S. Yuan, and H. Yong, CMOS RF and DC reliability subject to hot carrier stress and oxide soft breakdown, IEEE Trans Device Mater Reliab (2004), 92–98.
4. B.J. Lee, J.W. Park, K. Kim, C.G. Yu, and J.T. Park, Comparison of hot carrier-induce RF performance degradation in H-gate and T-gate SOI MOSFETs, IEEE Electron Device Lett 26 (2005), 112–114.
5. C.H. Huang, K.T. Chan, C.Y. Chen, A. Chin, G.W. Huang, C. Tseng, V. Liang, J.K. Chen, and S.C. Chien, The minimum noise figure and mechanism as scaling RF MOSFETs from 0.18 to 0.13 μm technology nodes, Digest of Papers-IEEE Radio Frequency Integrated Circuits (RFIC) Symposium (2003), 373–376.
6. M.C. King, M.T. Yang, C.W. Kuo, Y. Chang, and A. Chin, RF noise scaling trend of MOSFETs from 0.5 μm to 0.13 μm technology nodes, Digest-IEEE MTT-S Int Microwave Symp (2004), 9–12.
7. M.C. King, Z.M. Lai, C.H. Huang, C.F. Lee, M.W. Ma, C.M. Huang, Y. Chang, and A. Chin, Modeling finger number dependence on RF noise to 10 GHz in 0.13 μm node MOSFETs with 80 nm gate length, Digest of Papers-IEEE Radio Frequency Integrated Circuits (RFIC) Symposium (2004), 171–174.
8. H.L. Kao, A. Chin, B.F. Hung, J.M. Lai, C.F. Lee, M.-F. Li, G.S. Samudra, C. Zhu, Z.L. Xia, X.Y. Liu, and J.F. Kang, Strain-induced very low noise RF MOSFETs on flexible plastic substrate, Symp on VLSI Tech (2005), 160–161.
9. A. Chin, K.T. Chan, H.C. Huang, C. Chen, V. Liang, J.K. Chen, S.C. Chien, S.W. Sun, D.S. Duh, W.J. Lin, C. Zhu, M.-F. Li, S.P. McAlister, and D.L. Kwong, RF passive devices on Si with excellent performance close to ideal devices designed by electromagnetic simulation, Int Electron Devices Meeting (IEDM) Tech Dig (2003), 375–378.
10. C.-L. Lou, W.-K. Chim, D.S.-H. Chan, and Y. Pan, A novel single-device DC method for extraction of the effective mobility and source-drain resistances of fresh and hot-carrier degraded drain-engineered MOSFETs, IEEE Trans Electron Devices 45 (1998), 1317–1323.
11. C.T. Liu, E.J. Lloyd, C.P. Chang, K.P. Cheung, J.I. Colonell, W.Y. C. Lai, R. Liu, C.S. Pai, H. Vaidya, and J.T. Clemens, A new mode of hot carrier degradation in 0.18 μm CMOS technologies, Symp on VLSI Tech (1998), 176–177.
12. P.R. Gray, P.J. Hurst, S.H. Lewis, and R.G. Meyer, Analysis and design of analog integrated circuits, 4th ed., Wiley, New York, 2001. Chapter 11.

© 2006 Wiley Periodicals, Inc.

COMPACT LTCC BANDPASS FILTER DESIGN WITH CONTROLLABLE TRANSMISSION ZEROS IN THE STOPBAND

Jianhua Deng, Bing-Zhong Wang, and Tiguo Gan
Institute of Applied Physics, University of Electronic Science and Technology of China, Chengdu 610054, People's Republic of China

Received 4 March 2006

ABSTRACT: *Method of designing a modified Chebyshev bandpass filter with controllable transmission zeros in the stopband is described. A novel compact structure of this kind of filter with a transmission zero located at higher stopband for LTCC implementation is proposed. The filter has promising potential applications in miniaturized wireless communication systems.* © 2006 Wiley Periodicals, Inc. Microwave Opt Technol Lett 48: 1919–1922, 2006; Published online in Wiley InterScience (www.interscience.wiley.com). DOI 10.1002/mop.21814

Key words: *bandpass filter; LTCC; transmission zero*

1. INTRODUCTION

The emerging applications of personal communication networks, wireless local networks, satellite communications, and automotive electronics provide the impetus for the wireless electronics thrust. Small-size components of wireless communication module are extensively studied because the need for a small apparatus is